National Conference with International Participation

ENGINEERING MECHANICS 2008

Svratka, Czech Republic, May 12 – 15, 2008

MECHANO/FLUIDIC DEVICES EMPLOYING THE "AERODYNAMIC PARADOXON"

V. Tesař*

Summary: *A mechanism of aerodynamically excited vibration of a movable or elastic solid body was investigated and suggested for use in a number of fluidic (or mechano/fluidic) devices. The vibration is based on a phenomenon little known and so far practically not used, despite of its very old history. The effect leads to an alternating direction of a fluid force acting a movable object exposed to fluid flow. One of the directions is interesting: it is the very opposite to what an uninitiated observer may expect. Early investigations of this "paradox" by the present author in 1971 became recently of renewed interest because of the possible topical use in biosensors.*

1. Introduction: the phenomenon

This paper discusses an unusual operating principle of fluidic devices (e.g., Tesař 2007), mainly oscillators and sensors generating an oscillatory fluidic output, based on a little known and little used phenomenon of interaction between a moving body and a fluid stream. The phenomenon gives rise to periodic oscillation caused by alternating the direction of the force

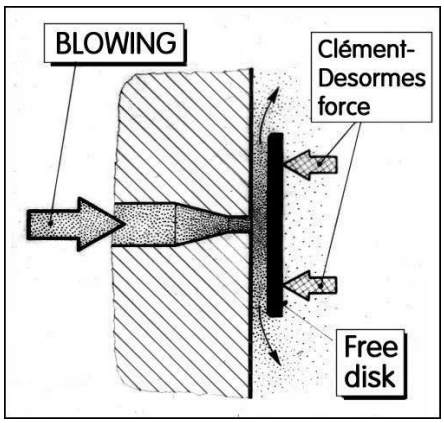

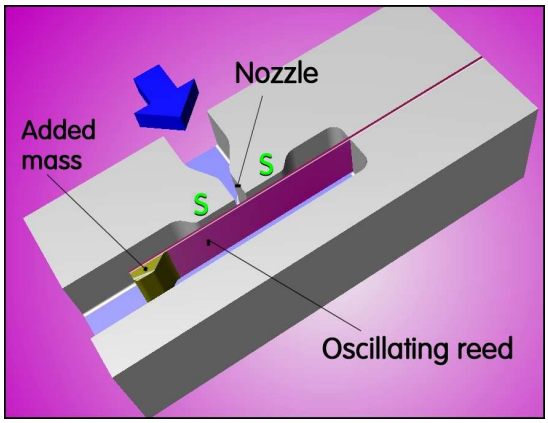

Fig. 1 (Left) The motion of a free disk towards the nozzle, opposite to the direction of the fluid flow from the nozzle, was first observed and described by Clément and Desormes already in 1827 and called by them "Aerodynamic Paradoxon". Analysis of the effect became available in literature much later, e.g. Paivanas & Hassan 1981.

Fig. 2 (Right) An example of a fluidic oscillator based on the "Aerodynamic Paradoxon" phenomenon. The free disk is here replaced by a reed fixed at one end. The motion is made possible by elasticity of the reed – which, however, brings additional elastic factors into the effect.

* Prof. Ing. Václav Tesař, CSc.: Institute of Thermomechanics AS CR v.v.i., Dolejskova 5, 182 00 Prague, Czech Republic, tel.: +420 266 052 270, e-mail: tesar@it.cas.cz

by which the fluid acts on the body. While one of the force directions is obvious, the body moving along with the fluid flow, the other is caused by an effect that is contrary to intuitive expectations. In spite of this effect being unfamiliar, it is by no means new – in fact, it was described in scientific literature already in 1827, earlier than most other aerodynamic phenomena. The scientists who encountered and investigated the effect 181 years ago were Nicolas Clément and his son-in-law Charles Desormes. They called this phenomenon "*Aerodynamic Paradoxon*" and under this name it may be found in literature, especially old one such as e.g. in Teyssler & Kotyška 1933. Of course, like all paradoxes in fluid mechanics, this phenomenon may be easily explained on the basis of standard basic principles. The effect was observed and demonstrated in several alternative configurations of qualitative experiments. Probably the least expected and therefore the perhaps most "paradoxical" is the case with a free disk located in front of a nozzle from which issues an air flow according to Figs. 1 and 3. An uninitiated observed usually expects the disk to move by the action of the air flow away from the nozzle in the direction of increasing distance X. In other words, a positive force D (Fig. 4) is expected. The actual motion of the disk is quite the opposite: it moves towards the nozzle, opposite to the direction of blowing air. This is because of the low pressure region that is generated between the disk and the surface S (Figs. 2, 3).

When the disk is moved this way to close the gap the air flow stops, being blocked by the disk. The pressure upstream from the disk increases. The resultant pressure force then tends to move the disk in the direction of positive distance X. The sign of the force D is changed and it becomes positive. Theoretically, the disk may remain in the stable equilibrium point shown in Fig. 4 - the point where the force D becomes zero. However, this equilibrium position is impossible to attain. Inertia of the disk usually moves it beyond the equilibrium thus generating a force that pushes it back. The alternating positive and negative action causes the disk to oscillate back and forth.

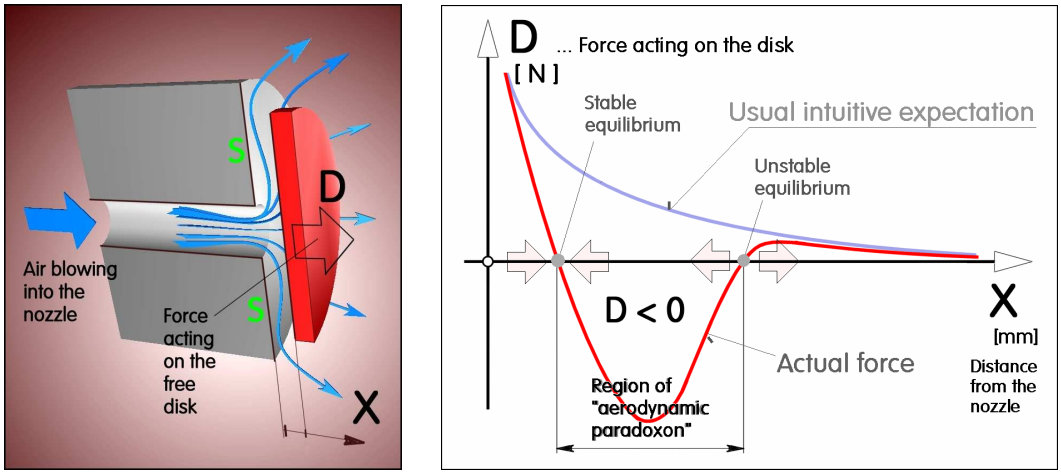

Fig. 3 (Left) In the space between the disk and the surface S (which surrounds the nozzle exit) the pressure decreases due to the conversion of a part of fluid pressure energy into the kinetic energy. This region behaves as a diffuser: the flow cross-sectional area increases in the streamwise direction. As in other diffusers, the pressure in the flow direction increases. Since it finally after the rise reaches the atmospheric value at the disk periphery, the pressure under the disk must be obviously lower than atmospheric.

Fig. 4 (Right) The negative pressure force acting on the disk may be in a certain region of distances X larger than the impact force which is positive (= acting in the direction which is intuitively expected). As a result, the total force D is locally negative. Disk placed there is attracted towards the nozzle.

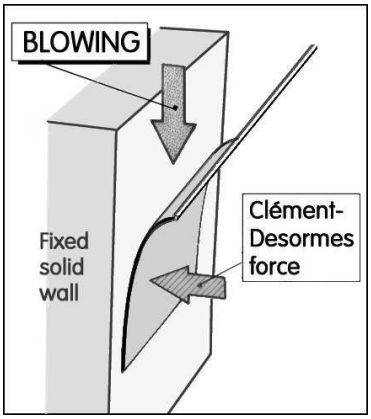

Fig. 5 (Left) Essentially the same "Aerodynamic Paradoxon" effect as in Fig. 1 is found with bodies or objects exposed to a flow that is not perpendicular but sometimes even tangentially directed towards the moving object. In this case the effect forces the movable end of a flexible foil towards the wall.
Fig. 6 (Right) A symmetric version with two sheets of paper, one of them replacing the effect of the presence of the wall in Fig. 5. Blowing into the gap, instead of moving the sheets apart as expected, forces them to come together - which blocks the flow, so that they are blown apart again.

Essentially the same "Aerodynamic Paradoxon" effect is found if instead of the flow initially perpendicular to the moving component, the air is blown on an inclined flexible or movable component reaching up to an opposite fixed wall, Fig. 5. Of course, the initial direction of blowing is immaterial; the low pressure is in Fig. 3 generated in a flow tangential to the disk surface, after the directional change associated with the initial impact flow. Again, one may perhaps intuitively expect the inclined movable component will be blown further away from the wall thus increasing the width of the passage available for the air. What actually happens is the opposite motion caused by the pressure force of the Clément-Desormes character, which moves the flexible component toward the wall. This effect is usually demonstrated as shown in Fig. 6 in a symmetric layout with two flexible components (paper sheets). Again, because of their inertia, the sheets do not remain in an equilibrium position and enter instead a regime of periodic oscillation.

The phenomenon of the "Aerodynamic Paradoxon" and the oscillation based on it were investigated by the present author quite a long time ago, already in 1971 – reference Tesař, 1971. At that time, no information about the details of the aerodynamics of the effect was available in literature – in fact the first analysis of the Clément-Desormes attraction force not known until 10 years later, Paivanas and Hassan 1981, and this actually assumed steady states, not the oscillation. Analysis of the oscillation phenomena, made complex by the impact of the reed or body on the contact wall, is so far not yet available. In existing references Tesař 1971, 1972 a to f, and 1976, the interest was not in understanding the mechanism, but in finding applications of the phenomenon in various fluidic devices. From theoretical point of view, there are still interesting aspects of the discussed phenomenon remaining a challenging opportunity for researchers.

2. Experiments with hinged metal foils – Two regimes N and M

In the demonstration experiment shown Fig. 8, the flexible paper foils of Fig. 6 are replaced by the curved sheet-metal foils movable on hinges. The hinges were oiled to reduce the friction. The oscillatory motion of foils is so intense they hit at one another and bounce at

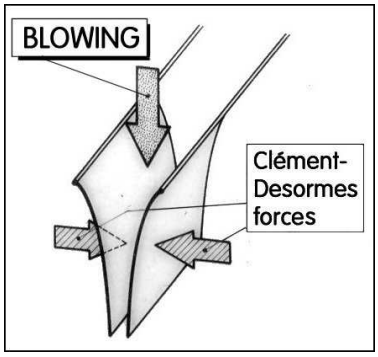

Fig. 7 (Left) A symmetric oscillator driven by the two alternating pressure effects: the "Aerodynamic Paradoxon" moves the two hinged or elastic foils together. This blocks the flow and causes a pressure rise upstream – so that the foils are blown apart. They overshoot and the "Aerodynamic Paradoxon" drives them together again. Thus the foils are kept in flapping motion, with their ends periodically coming to a contact.

Fig. 8 (Right) An oscillator model with two hinged solid duraluminium foils. Geometry of the foils is presented in Fig. 9. Oscillation frequency could be easily measured by counting the periodically interrupted metallic contact.

the end of their inward motion in each cycle. The experiment, Fig. 10, was conducted to reveal quantitative aspects. The metallic contact in each cycle made the frequency of oscillation easily measurable electrically. Of course, the mechanics of the percussion made the oscillation so difficult to analyse that no useful theoretical model could be made. The geometry of the experiment is shown in Fig. 9. The rather large (note the 70 mm span in Fig. 9) and relatively heavy foils hung down from their hinges. They could be put into intense

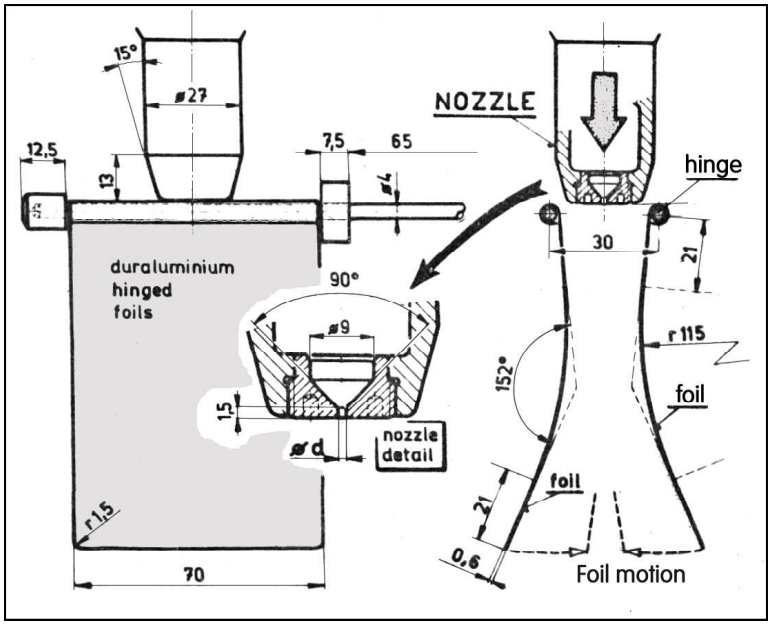

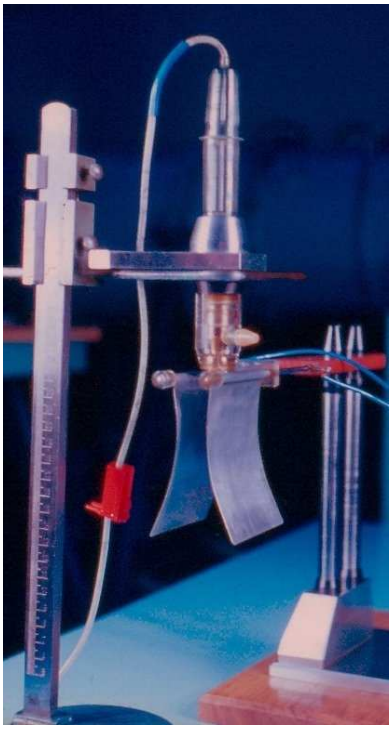

Fig. 9 (Left) Details of the geometry of the experiment shown in Fig. 10. Note the very small d = 1 mm diameter of the nozzle exit.

Fig. 10 (Right) Photograph of the experiment with the two hinged solid foils. They hang down from their horizontal hinges. An air jet is blown from the nozzle between them.

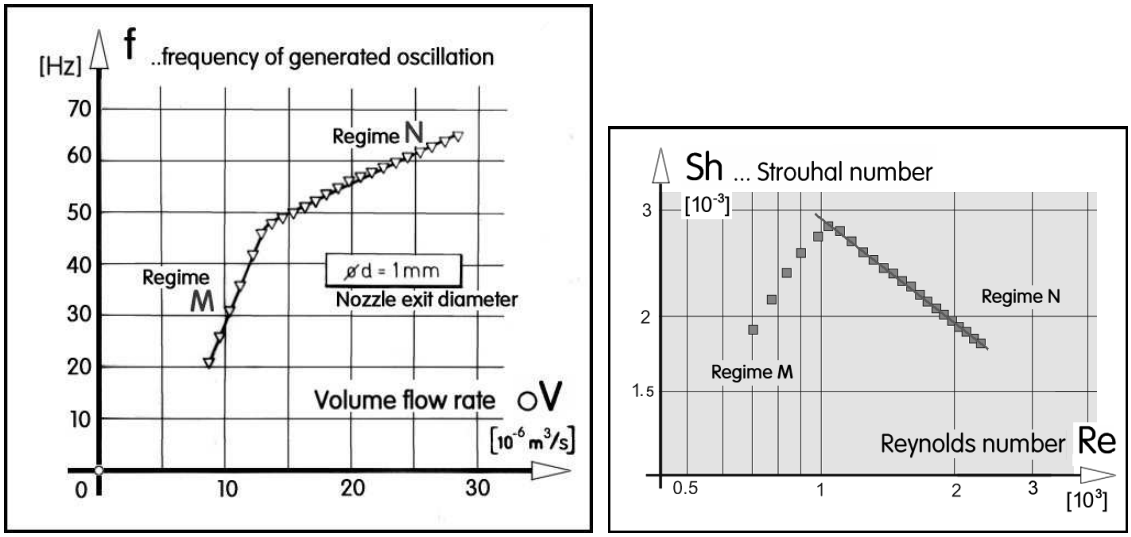

Fig. 11 **(Left)** Measured oscillation frequency in the experiment with the hinged duraluminum foils oscillator as shown in Figs. 8 to 10. The dependence on the nozzle air flow rate may be well fitted by straight lines, with clearly recognisable transition between them: the initial regime M with steeper slope changes at higher flow rates into another regime N.

Fig. 12 **(Right)** The experimental results from Fig. 11 re-plotted as the dependence of Strouhal number on the nozzle exit Reynolds number.

oscillation by a quite weak downwards oriented vertical air jet, issuing from a small nozzle of 1 mm exit diameter. The measured dependence of oscillation frequency on the nozzle flow rate was found to be somewhat surprising, as shown plotted in Figs. 11 and 12. As is generally known, typical for oscillation of fluid flows past (or through) constant-geometry object is a simple proportionality between the flow rate and the oscillation frequency – or, in other words, a constancy of the Strouhal number Sh. This is not the case here. In the investigated range of flow rates, there are two different regimes, called regime M and regime N in Fig. 11. In both, the dependence could be well fitted by linear functions, but there is no simple proportionality - neither one of the two linear functions passes through the origin. The cause behind the transition from M into N was not identified.

.

3. Experiment with elastically supported moving body

In an attempt to reduce the complication cause in the oscillation mechanism by the friction in the hinges, an alternative was sought in supporting the moving body by elastic oscillating components. To reduce further the complexity, solid (not changing their shape during the cycle) foil-shaped bodies were used. The shape was chosen so as to provide a local flow cross-section contraction, producing the local decrease of pressure. In the configuration actually tested, shown in Figs. 13 and 16, only one oscillating contraction body is used, fixed at the free (oscillating) end of a steel strip. The other end of the strip is fixed in the clamp. To investigate the influence of the elastic forces introduced by the presence of this strip, the free length l of the strip (Fig. 13) could be adjusted.

Results of the experiment with this model are presented in Fig. 15, similar to the previous Fig. 11 above. There is again the volume flow rate on the horizontal co-ordinate and the frequency of oscillation plotted on the vertical axis. In fact, also the character of the dependences found for the model from Figs.13 and 14 is to some degree similar – which may

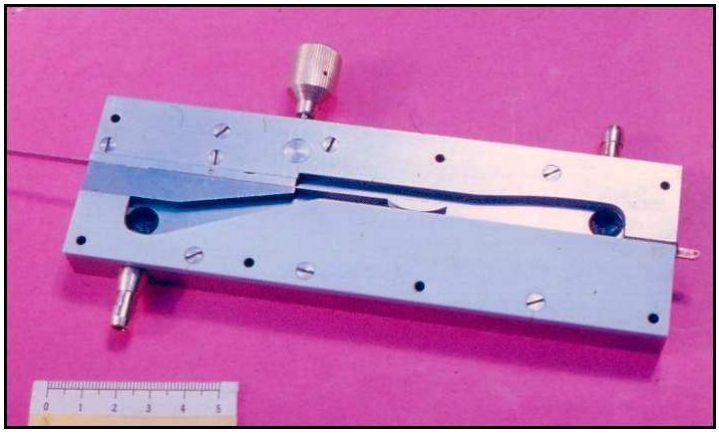

Fig. 13 The oscillator model used in experiments with asymmetric, one-foil (cf. Fig. 5) version of the "Aerodynamic Paradoxon" effect, with the "foil" held on flexible spring replacing the hinge. The spring or reed is formed by of a steel strip the oscillating part of which may be adjusted to different lengths *l* . The "foil" is actually a somewhat massive contraction body; the details of the geometry are presented in the next Fig. 13.

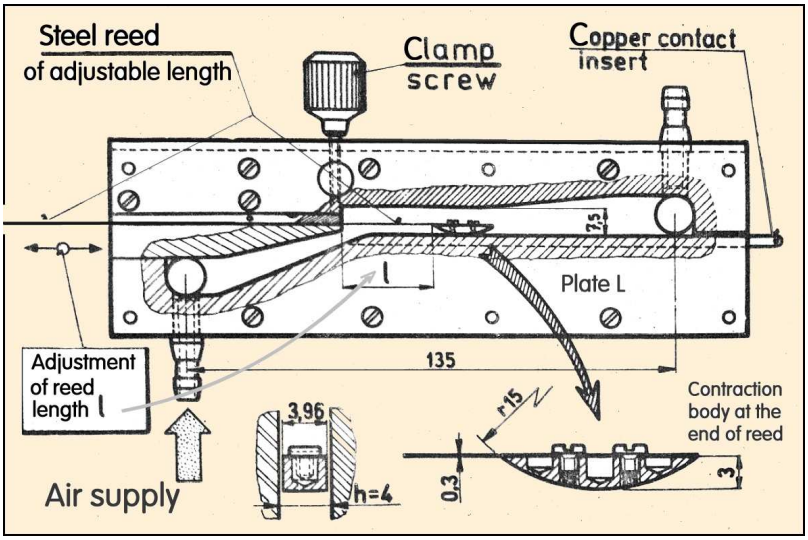

Fig. 14 Drawing of the oscillator model from Fig. 13. The fixed solid wall (cf. Fig. 5) is formed by the electrically non-conducting plate L with inserted contact strip so that oscillation frequency could be measured by counting the periodically interrupted contact with the contraction body.

be surprising, considering all the differences between the two designs. As the flow rate is increased, there is first a region with a steeper slope, corresponding to the regime M, and then at higher flow rates a transition into another regime with frequency less dependent on the flow rate – this may be seen as corresponding to the regime N from Fig. 11. The two regimes, M and N are now separated by a distinct local maximum of frequency. This maximum is more pronounced at shorter free lengths *l* . This is where the elastic forces in the deformed steel spring band play a more important role. It should be also noted that the sloping part ("region M") in Fig. 15 might be, with some tolerance, seen as not far from passing through the origin and this region may be therefore more akin to constant Sh aerodynamic mechanism. The peak — which is perhaps even more pronounced in Fig. 16 presenting the dependence between Sh and Reynolds number — may be seen as being associated with some form of elastic resonance. After the transition, the frequency f of generated oscillation tends to be near to constant – and this is particularly the case at longer free lengths *l*. This is of im-

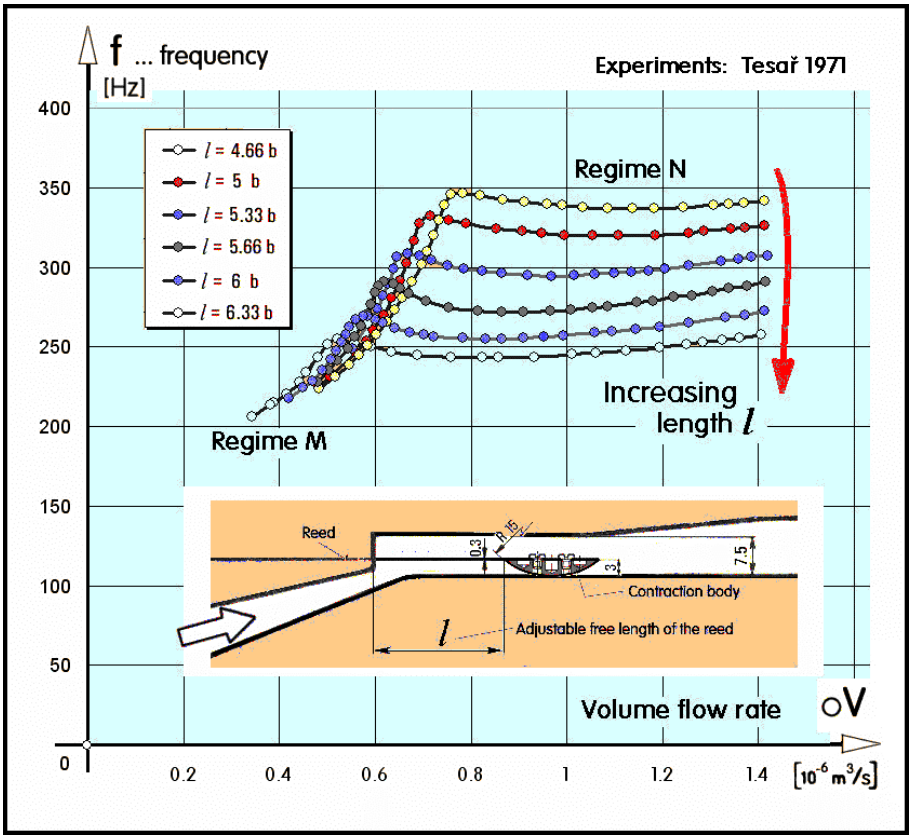

Fig. 15 The dependences of the oscillation frequency on the supply air flow rate found in experiments with different lengths *l* with the model from Figs. 13 and 14. Each line in this diagram was obtained for a constant particular length *l*. Each exhibits the transition analogous to the change of the initial regime M into the regime N in the experiments shown in Fig. 11.

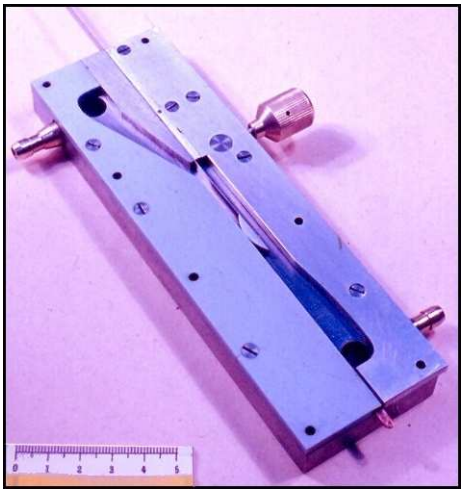

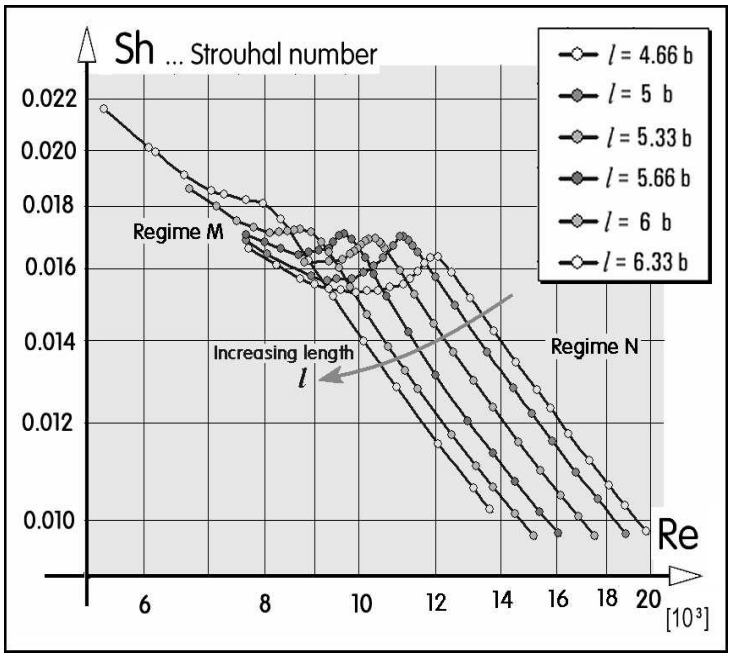

Fig. 16 **(Left)** Another photograph of the experimental model corresponding to the drawing in Fig. 14..
Fig. 17 **(Right)** Results from Fig. 15 converted into the dependence between Strouhal and Reynolds number and plotted in logarithmic co-ordinates. The dominant feature is again local maximum of values at the transition between the regimes M and N.

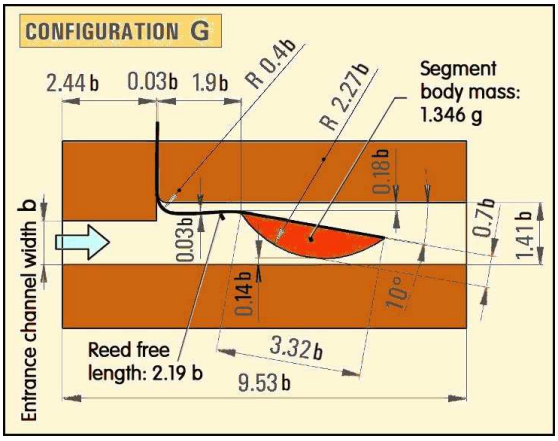

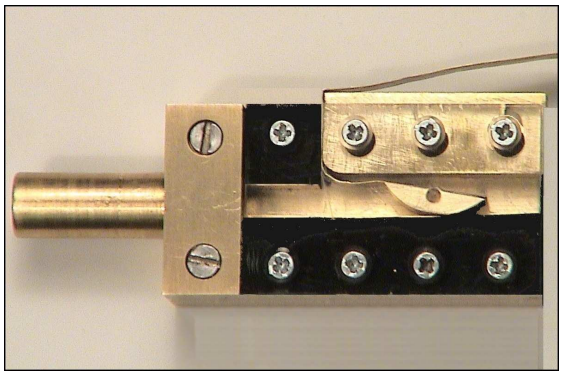

Fig. 18 **(Left)** One of the alternative model geometries investigated recently in association with the renewed interest in the phenomenon.

Fig. 19 **(Right)** Photograph of the laboratory model used in the tests with the spring-supported contraction body (Figs. 18 and 20). In this case, the contraction body held as in the configuration G (Fig. 18) has its mass decreased, like the configuration H, by drilling the hole.

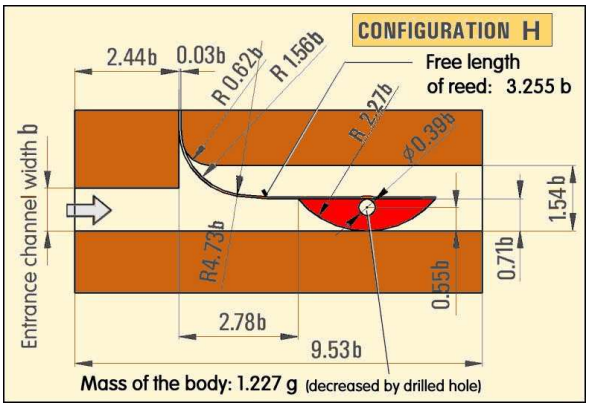

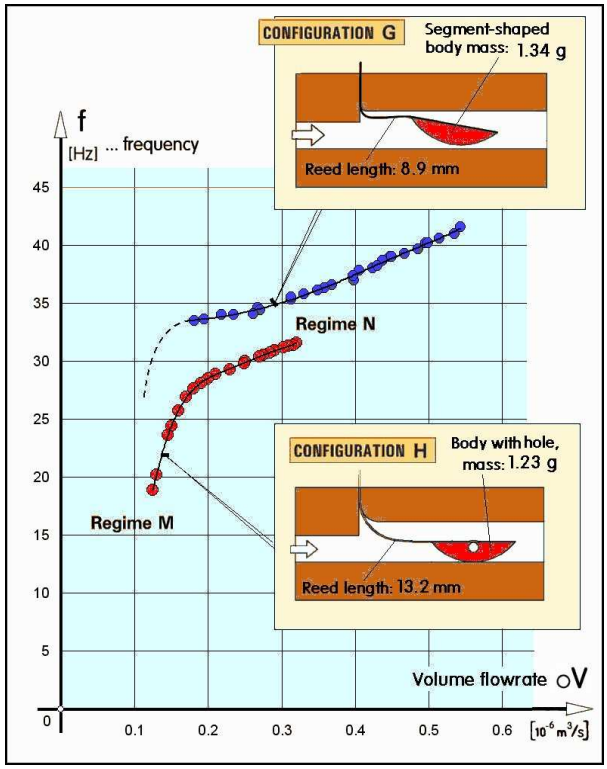

Fig. 20 **(Left)** Details of the other of the alternative geometries in the experiments with the spring-supported contraction body.

Fig. 21 **(Right)** The transition between the regimes M and N or a trend towards such a change could be observed also in the experiment with the configurations from Figs. 18 and 20. In the configuration G, the signal generation failed just in the region where the transition could be expected.

portance for the discussed applications in fluidics, where a constant frequency, not varying with changes in the supply flow rate, is a distinct advantage over the no-moving-part fluidic oscillators with their typical frequency increase with increasing flow rate.

In the period since the author's first demonstrations of the oscillation based on the "Aerodynamic Paradoxon" some investigations were made in particular of this case of the tangential blowing on a curved contraction body, supported by a flexible spring, in a channel. Shapes similar to those in Figs. 13 and 17 became of interest because of the similarity to the problem of vocal cord total prostheses. The "reeds" used in these investigations, however, were inelastic, of polymeric materials. Very recently, an interest into the Clément-Desormes force has led to interesting stability studies, cf. e.g. Antoine, Hermona and de Langre, 2008. Repeated verification tests were performed with the models shown in Figs. 18 and 20 (the photograph in Fig. 19 shows another version). In the configuration G, small-amplitude oscillation could be detected around the stable equilibrium point (Fig. 2) with the contraction body not contacting the wall. This, of course, made impossible measuring the frequency just in the range where the interesting M -N transition could be expected. Nevertheless, the existence of the transition as well as the existence of the local extreme could be clearly demonstrated with the other configuration H (Fig. 21).

4. Fluidic oscillators with the reed

4.1 A simple two-terminal version – with electric output

After the hinged and spring-supported contraction bodies, yet another configuration of direct interest in fluidics was investigated. I this case, the movable body was just the thin reed – Fig. 23. The aerodynamically desirable contracting shape was made by bending, a relatively large radius, of the free end of the reed. This idea was tested in the oscillator (and fluido/electric transducer) made by traditional manual manufacturing procedure – of geometry specified in

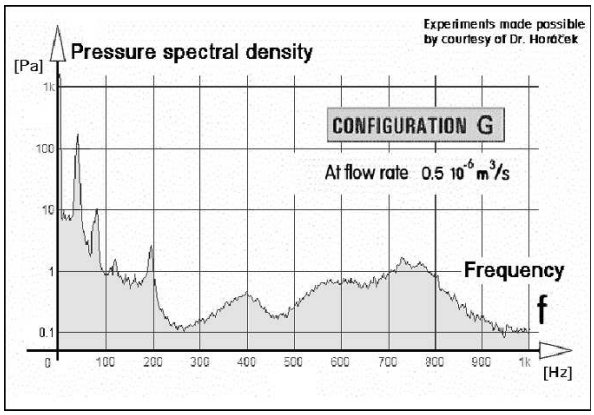

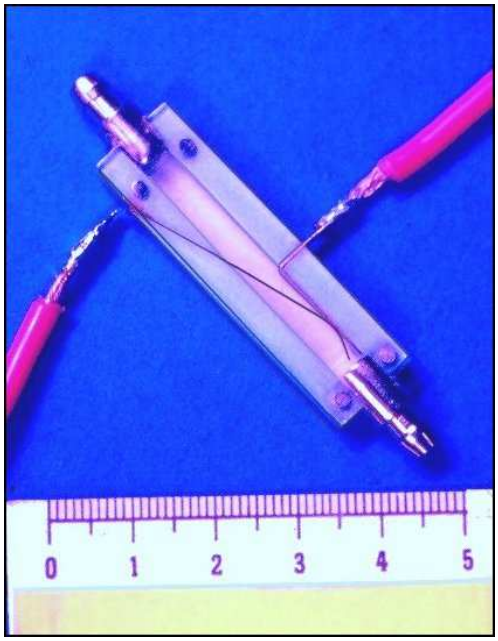

Fig. 22 **(Left)** Frequency spectrum of the acoustic signal generated by the oscillator configuration G. Note the logarithmic vertical scale: the spectrum is actually dominated by the first peak maximum.
Fig. 23 **(Right)** Fluidic oscillator model with vibrating reed driven by the air flow supplied through the upstream ferrule. The two electric terminals produce an electric pulse each time the reed contacts the metallic strip on the channel wall.

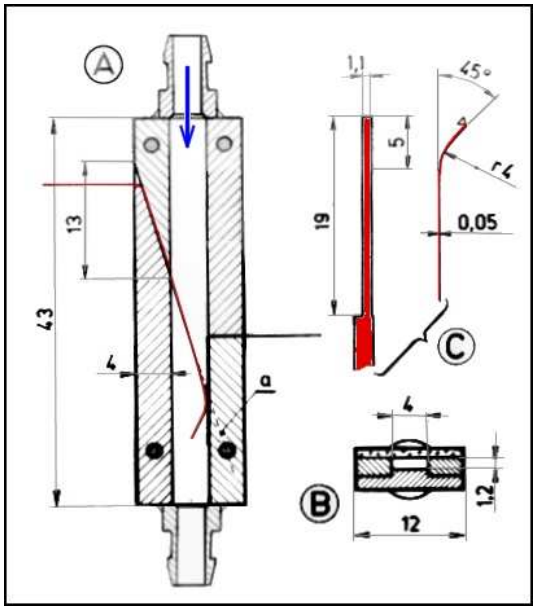

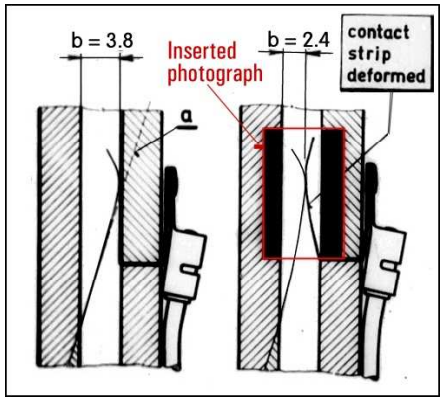

Fig. 24 **(Left)** Drawing of the oscillator presented in Fig. 28. The three part of this drawing are: A the plan view, B the cross section (note the 4 mm x 1.2 mm channel cross section), and C a drawing of the phosphor bronze reed.

Fig. 25 **(Right)** Drawings of the standard reed shape of the device in Figs. 23 and 24 and – at right, with inserted photograph frame (inside the red box) - of the deformed metallic contact strip opposite to the reed. The deformation decreased the available channel width and also pre-stressed the reed, which resulted in an increase of the frequency of the generated oscillation.

Fig. 24. Again, the results of the investigation (in the form of dependence of the frequency of the generated oscillation on the driving pressure) are presented in Fig. 26.

Perhaps significantly, even here the behaviour is not monotonous and there are two different recognisable regions, resembling the two regimes M and N. The frequency was measured by a counter, sensing the electric pulses generated when the end of the reed contacted the fixed metallic strip at the opposite wall. The tests involved bending this strip (Fig. 25) so that the increased pre-stressing of the reed as well as the increased flow velocity in the smaller cross section has increased the frequency – Fig. 26.

In both configurations, at the lower part of driving pressure range of values, perhaps corresponding to the regime M, the frequency was observed to increase in a practically linear manner with the pressure drop. In this regime, the device could be evidently used as a flowmeter with frequency-coded output. This sort of output is, of course, particularly suitable for digital processing of the measurement results. The fitted straight lines, again, unfortunately do not pass through the origin of the diagram, the device is less sensitive than the purely aerodynamic constant Sh flowmeters. Moreover, after the transition – which for both configuration took place at about the same pressure drop ~7.5 kPa – this regime was replaced by what is very nearly constant- frequency mode of operation.

The flow rate of air passing through the device was also measured so that it were possible to compute the Strouhal number and plot it against the Reynolds number, as is done in Fig. 27. A rather surprising results of this way of processing the experimental results shown there is the fact that the data for both configurations may be fitted by practically a single straight line. As was already mentioned above, this regime may be also quite useful. There are applications of fluidics in which the constant frequency is needed. Other solutions of

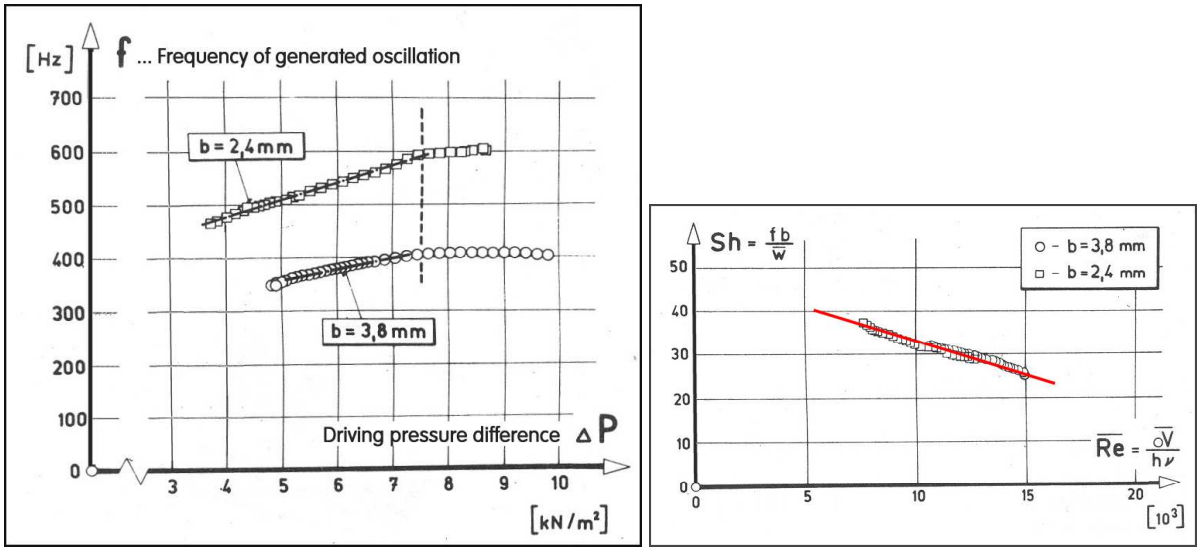

Fig. 26 **(Left)** Experimental data on the dependence of the generated frequency on the driving pressure for the two geometries shown in Fig. 30. There are again two regimes and a distinct transition between then: the initial sloping dependence (frequency increases with increased pressure difference) is at large driving pressures replaced by a constant frequency regime.

Fig. 27 **(Right)** An interesting relation between the two results shown in Fig. 31 for the two different geometries. When plotted as the dependences of the Strouhal number Sh on the rime-mean Reynolds number (evaluated from the time-mean volume flow rate through the device), the widely different relations tend to convert into what is practically a common straight line.

mechano/fluidic oscillators, based on locking-in of the oscillatory process to a mechanical oscillator — such as, e.g., a tuning fork – are known, but their practical realisations are complicated and difficult to manufacture. In particular, driving the fork requires a fluidic amplifier with mutual crossing of the feedback channels leading to the opposite sides of the free end of the fork (or, for that matter, a simple cantilever) which necessitates making the device not planar, but as an assembled three-dimensional structure. The configuration according to Fig. 24, with the self-excited oscillation of a simple reed exposed to the flow is perhaps the simplest way how to design the mechano/fluidic oscillator.

4.2 **A three-terminal multi-purpose device**

Presented in Figs. 29 and 30 there is an example of a small fluidic laboratory model device made manually by classical methods: drilling in a polymethylmetacrylate (plexiglass) plate (thickness 2.4 mm) and gluing into it a reed made from thin sheet of phosphor bronze. In this case, the reed is pre-stressed so that it starts to oscillate only after applying a rather high pressure.

Essentially, the idea behind this design is replacing the electric contact of one moving and one fixed conductors by its fluidic equivalent: closing an orifice in a wall by a moving component when it at the end of its motion comes into contact with the wall. This, instead of generating the electric pulses generates fluidic pulses. Alternatively, the configuration may be seen as having two air inlet terminals. There is a choice between generating the oscillation of the reed either by the normal blowing mechanism (corresponding to Fig. 1) or by the tangential (corresponding to Fig. 5). Tests with these two different regimes, as presented in

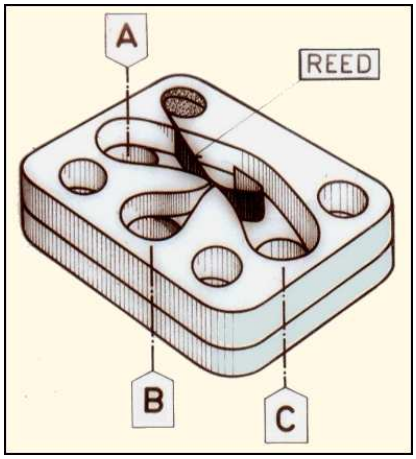

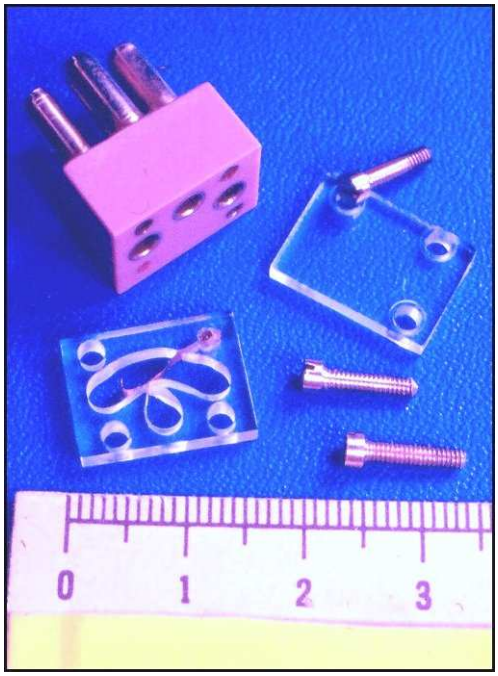

Fig. 28 **(Left)** Original drawing of a multi-purpose mechano/fluidic oscillator from the Patent document, Tesař & Balda 1972. The terminal B may serve either for driving the reed (by the Clément-Desormes mechanism, Figs. 1 and 3) or as an output terminal with zero flow rate between the pulses. It may also serve as the control terminal or as an output.
Fig. 29 **(Right)** Photograph of the disassembled model used by the author in the verification tests of the idea from Fig. 28..

Figs. 31 and 32, revealed in both cases a linear dependence of the frequency on the driving pressure difference. In the tangential flow mode, Fig. 31 (from the terminal A), the slope of the dependence is lower, 7.6 Hz / kPa while in the perpendicular impact mode, Fig. 32 (air flow from the terminal B, corresponding to the original Clément-Desormes mechanism, Figs. 1 and 3), the slope is significantly higher, 11.5 Hz / kPa.

The device, with its key part as shown in Fig. 15 (again in operation actually covered with top and bottom cover plates) can also use the terminal B as an output. The advantage in relation to taking as the output the terminal C is the better the quality of the output waveforms available at this terminal B, which is completely closed by the reed during a part of the cycle so that the flow pulses have a zero flow rate between them (while inevitable free space on both sides of the reed, enabling it to move, cause a non-zero flow between the generated pulses. In yet another use of this device, the terminal B may serve as a control port. A fluidic control signal, is fed into B, changes the frequency of oscillation generated by the supply flow through the terminal A. The dependence of the frequency of generated vibration on the two pressure levels is presented in Fig. 33. It is rather interesting that the limit of the aperiodic behaviour (below which the device ceased to oscillate) is the frequency – the critical value of which was 340 Hz.

In view of the obvious usefulness of tuch a device, a question may arise as to the relative merits of the purely fluidic, no-moving-part devices. Of course, the devices with a reed may seem to be of limited life. The reed obviously is a vulnerable component that may be broken off due to material fatigue In laboratory tests with the device shown in Fig. 30, the reed was operated for $28 .10^6$ cycles, beyond typical total cycles limits of typical material fatigue, thus demonstrating there need not any be fears of limited life of the moving component.

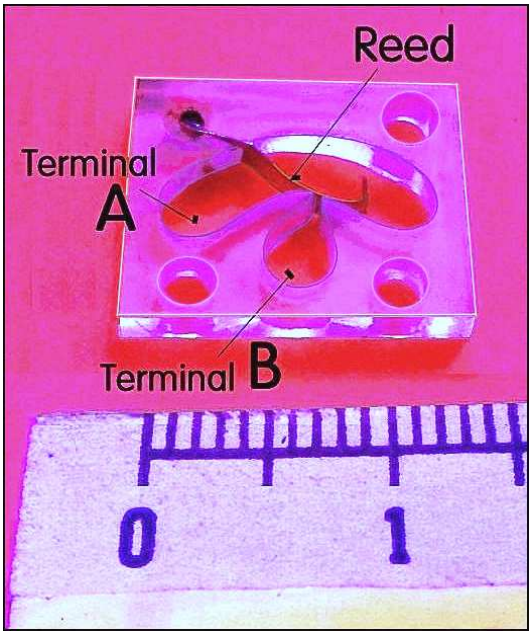

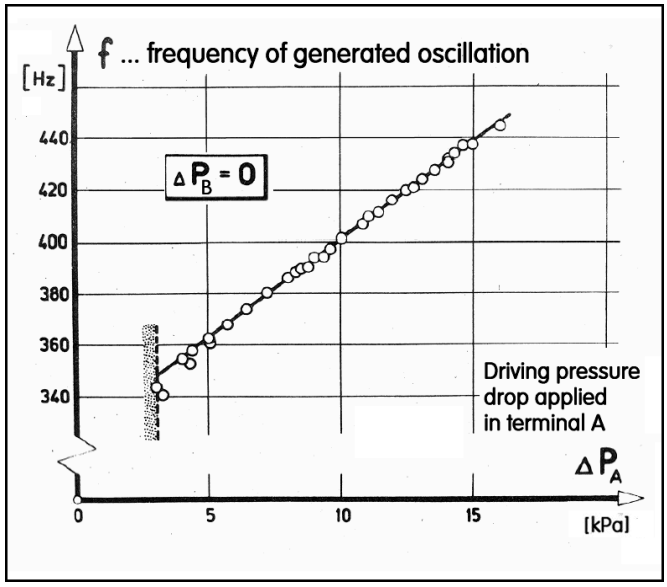

Fig. 30 **(Left)** The multi-purpose fluidic oscillator model. The oscillation may be generated by supplying the air flow either into the terminal A, when the operation corresponds to the one shown in Fig. 5, or into the terminal B, when the operation corresponds to Fig. 1.

Fig. 31 **(Right)** Measured frequency of the generated oscillation in the model shown in Figs. 23 and 24, plotted as a function on the pressure of the air supplied into the terminal A. The exit as well as the other input terminal B were open into the atmosphere.

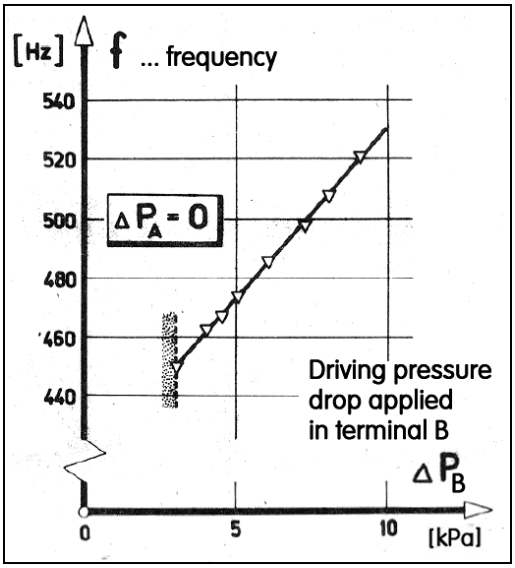

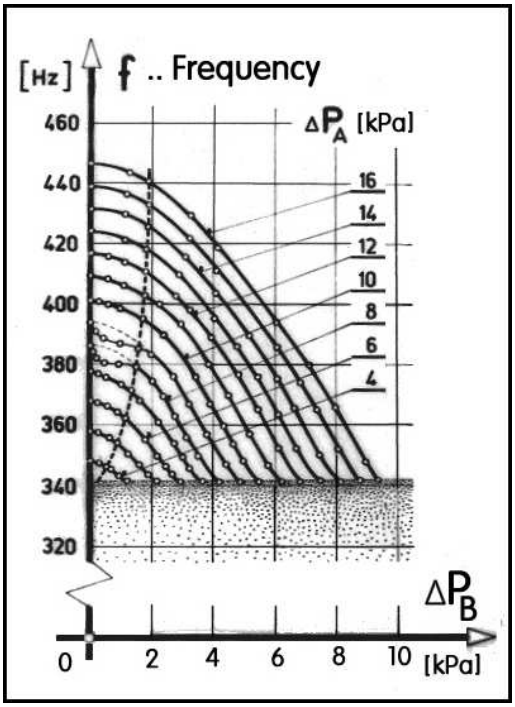

Fig. 32 **(Left)** Measured frequency of the generated oscillation in the model shown in Figs. 23 and 24 as a (rather surprisingly linear) function on the pressure of the air supplied into the "Clément-Desormes" terminal B. In this experiment, it was the exit and the other input terminal A that were open into the atmosphere.

Fig. 33 **(Right)** An example of the results obtained with the model shown in Fig. 24 with the terminal B used to control the frequency of the oscillation generated by the main flow supplied into the terminal

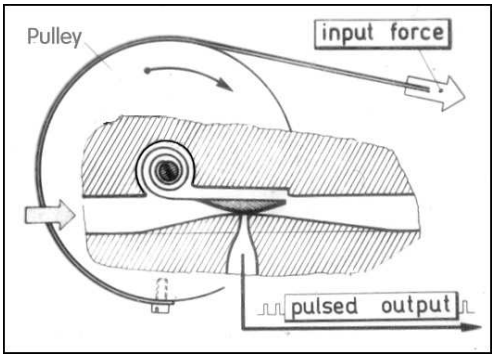

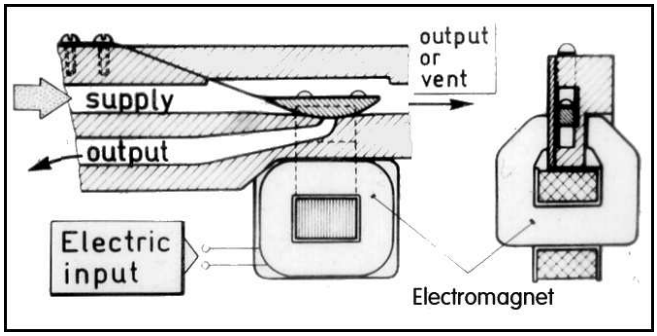

Fig. 34 **(Left)** An example of an illustration from an old Patent document (Tesař, 1972b) showing a possible configuration of a fluidic sensor of a mechanical input. The measured force is coded in the frequency of the output pulse signal. The frequency increase is due to pre-stressing of the spiral spring that holds the contraction body.

Fig. 35 **(Right)** Transducer for inputting electric signal into the frequency-coded fluidic output (also an old Patent drawing: Tesař, 1972a). The oscillation frequency is influenced by the electromagnetic force acting on the contraction body. Equally as in Fig. 33, the output from the terminal closed between the pulses by the contraction body generates a better quality of the output signal (zero flow rate between the pulses). Essentially the same device (without the third fluidic terminal) was tested to generate electric current for supplying electrical instrument at inaccessible location with ample fluid flow.

5. Transducers and sensors

The presence of the moving component in the fluidic device brings a possibility of the operation influenced by acting on this component by various non-fluidic forces. This changes the device into a conversion device (Chapter 5 in Tesař, 2007). The action results in changing the frequency of the generated oscillation – which is a particularly useful sort of output. Tests already made included sensors of mechanical input variables (force, motion) with the oscillator frequency changed by the input force stressing the elastic reed (Tesař 1972c), Fig. 34. The change in frequency in the stressed reed is directly related to the similar change produced by squeezing together lips or vocal chords. Other M/F (= mechano/fluidic) sensors with the mechanical input vary the geometry of the channel in which the reed vibrates (Tesař 1972e, 1972g). The favourable feature of the force sensor version according to Tesař 1972g – shown in Figs. 35 to 37 - is the high mechanical input impedance, i.e. very small deformation motion of the component on which the sensed force acts. The prototype model shown here was intended for use in measuring the forces acting on a model in a wind tunnel. The small deflection was important in that application because it assured constant position (e.g., a constant angle of attack) of the model.

The advantage of the frequency-modulated character of the output signal is it property of not being influenced by such disturbance effects like the inevitable hydraulic losses in the transmission pipes and tubes. This character of the output signal is, of course, and eminently suitable for subsequent digital processing. This advantage also applies to the temperature (T/F) sensor with bimetallic reed described in Tesař (1972a) and shown in Fig. 34 and the electric and/or magnetic E/F transducer (actually using conversion chain E/M/F) with electric input and fluidic output using magnetic force on a ferromagnetic vibrating body (Tesař 1972b). Of course, operation in the regime of frequency dependent on flow rate (regime M, Figs. 11 and 15 or the pressure dependence Fig. 31 or (differently operating) Fig. 32 can generate the advantageous frequency-modulated output signal dependent on the fluid conditions as the input. An interesting use in a device with a pair of differently tuned

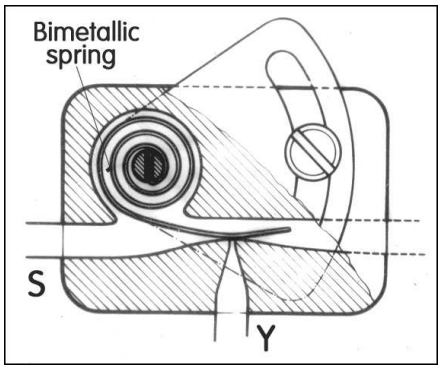

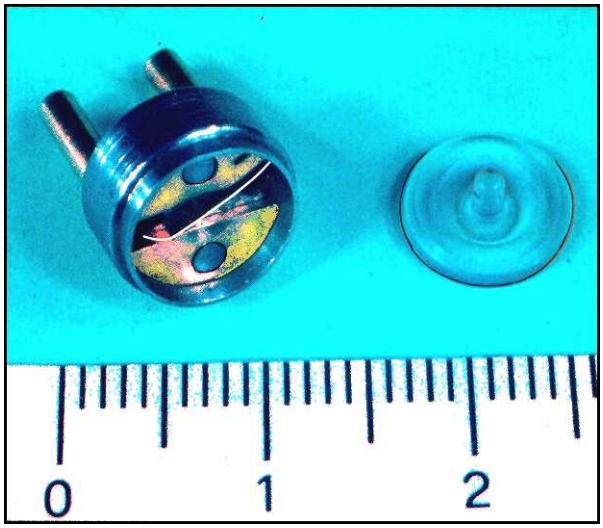

Fig. 36 **(Left)** Another variable-frequency oscillator sensor: mechano/fluidic sensing of fluid temperature useing a bimetallic reed, the free end of which oscillates. Because of the relatively large thickness of the bimetal strip, the reed is arranged in a spiral to increase its length a this decrease the oscillation frequency. The sensing is based on pre-stressing the reed a this way (cf the similar effect of frequency increase in Fig. 25 and 26) changing the oscillation frequency. Additional adjustable mechanical pre-stressing is used to set the frequency corresponding to the desirable temperature (Patent drawing, Tesař 1972e).

Fig. 37 **(Right)** Prototype of a force sensor with frequency-modulated output made by standard mechanical machining. The measured force deforms the Perspex lid (shown removed at right) and thus changes the flow allowed to by-pass the reed on one of its sides – Tesař 1972f.

oscillating reeds described by Tesař (1972c) for demodulating the frequency-modulated signal. The principle of oscillation generation may be actually used to perform the opposite task – to convert a fluidic input signal to some different output. The device already discussed above, the one with the electric current interrupting contact pair (one contact at the wall, the other one being the reed, Tesař 1971), as shown in Fig. 23, when operating in the variable

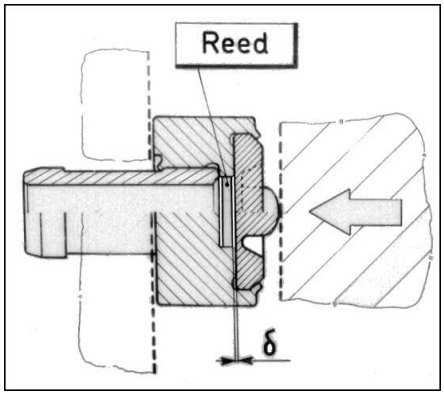

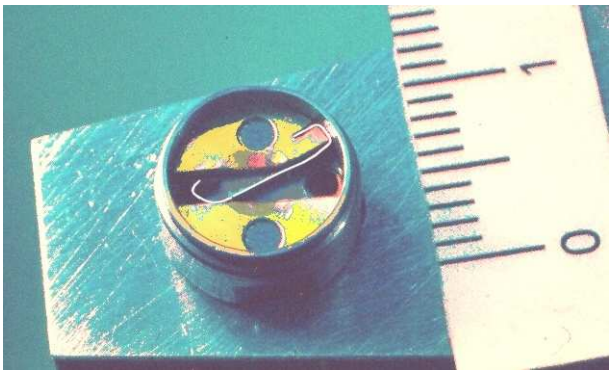

Fig. 38 **(Left)** Sectioned drawing of the force sensor (a slightly different layout, not the same as shown in the accompanying photographs of the prototype). There is a slot (of width δ) between the deformable lid and the edge of the reed, through which some fluid can pass. Deformation of the lid decreases the slot width; the reed responds by oscillating at a higher frequency.

Fig. 39 **(Right)** Another photograph of the force sensor prototype from Figs. 37 and 38. It was developed for use as a pneumatic force sensor for aerodynamic testing in wind tunnels..

frequency regime M is in principle also a transducer performing F/E conversion. Another device, the one according to Tesař (1972a) the electromagnet and the contraction body moving in its magnetic field, may be used (in the inverse conversion chain F/M/E) for electricity generation in otherwise inaccessible locations. It was investigated for the task of generating power for electronic in downhole bore locations. Perhaps the most interesting case among the tested conversion devices with fluidic input and a different output was the extremely simple, low-speed, low-power pneumatic or hydraulic motor (Tesař 1976). It was at one time considered for bomb activation (removal by the input air flow of a mechanical stop in front of the firing pin). This is described below in a separate paragraph.

6. Microfluidics: proposed monolithic version with an etched reed

Typical for present-day small scale microfluidics are devices – and whole fluidic circuits, consisting of sometimes a large number of mutually connected devices – made by the micromanufacturing methods. These were originally developed for producing microelectronics. A typical such manufacturing method is the removal of material from the surface of a planar substrate by etching. The original isotropic etching, unfortunately not suitable for producing deep narrow channels which would be better suitable for fluidic purposes, has been developed into much more sophisticated processes. The devices described in previous sections of this paper were mostly originally devised in early days of fluidics, where the components were rather large and were not considered for manufacturing by the progressive current methods. The idea of inserting into the channel the contraction body and its supporting reed as a separately made component were at the time quite acceptable – but in microfluidics this would be out of question. It is nowadays desirable to avoid any assembly operation and if possible to make even the "Aerodynamic Paradoxon" oscillators in a single etching production step. This calls for all the components designed in a monolithic form, with all parts made simultaneously by etching from a single substrate.

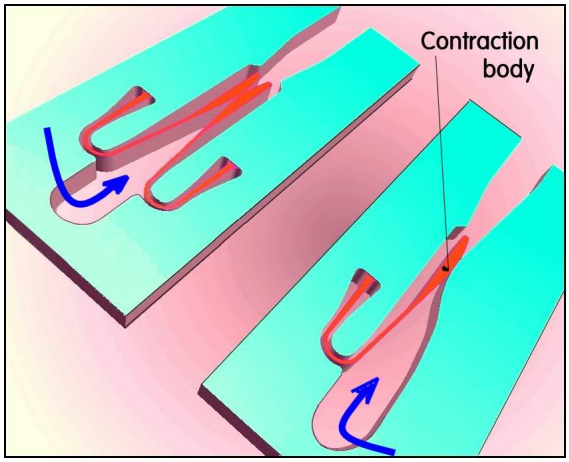

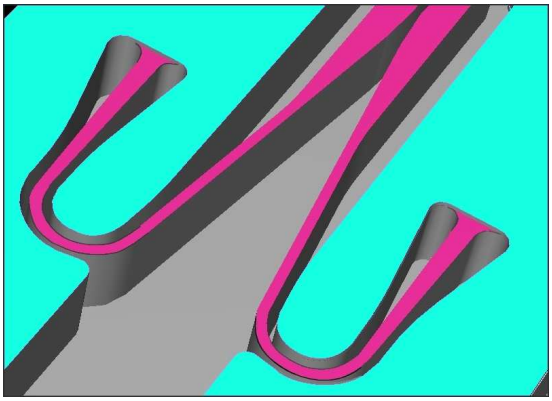

Fig. 39 **(Left)** Possible layouts of micro-scale versions of the "Aerodynamic Paradoxon" oscillators – with their elastically supported contraction bodies on a reed made together with the rest of the main part of the device by etching in a thin plane plate. Left upper corner shows a version with two contraction bodies (corresponding to Fig. 7) , right bottom corner a version with single body (Fig. 5).

Fig. 40 **(Right)** Detail of the roots of the reeds. The increased length is necessary to counter the otherwise too high reed stiffness dictated by the relatively very thick reed impossible to scale from the thickness used in the large-scale models.

The accompanying illustrations Figs. 39 and 40 show one possibility how such microfluidic oscillators with integral vibrating parts can me designed. The main problem is the impossibility of scale down to the microdevice size the reeds, already very thin even ib the large-scale microfluidic oscillators. To counter the too high oscillation frequency, associated with the thicker "reeds", it may become necessary to increase the reed length. Actually the same basic principle of a longer length, convoluted so as not to increase the overall size of the devices, was solved in the case of the sensor presented in Fig. 36. The full spiral used there would be perhaps too complicated in the microscale, but the shapes in Figs. 39 and 40 are a step in the same direction.

7. Recent development: a biosensors based on immunity reaction

One of the main reasons behind the present renewed interest is the proposed use of the oscillator based on the “Aerodynamic Paradoxon” phenomenon in increasing the effectiveness of sensing biological pathogens – and other particles carried in a fluid, such as protein molecules. The extremely important mechanism used in the detection procedure is the immunity reaction. This utilises antibodies – proteins generated by immunity systems of organisms for identification and capturing of antigens. These are the foreign objects, such as bacteria or viruses and other pathogens harmful for the organism. The reaction between an antigen and the antibody is very specific, there is usually no response even to very closely related antigens.

In a biosensor, the antibodies are immobilised on a detection surface. They are commercially available: earlier, they used to be produced by utilising the natural immunity system of animals (rabbits exposed to a particular pathogen), but this is nowadays replaced by humanly more acceptable production by genetically modified bacteria. The fluid possibly containing the corresponding antigens is left to flow past this surface. If the antigen is present

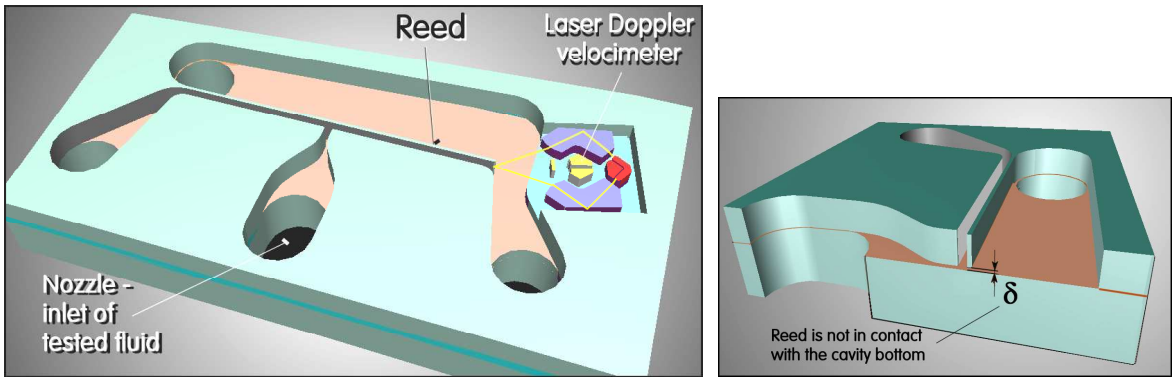

Fig. 41 **(Left)** A proposal of a biosensor based on the "Aerodynamic Paradoxon" oscillator. The antibodies are immobilised on the surface of the reed facing the exit of the supply nozzle. By the mechanism described above in association with Figs. 3 and 4, the reed is put into oscillation, the frequency of which is detected by the integral optical system corresponding to a laser Doppler velocimeter. Capturing the antigens on the reed reduces the frequency and this is immediately recognised in the velocimeter response.
Fig. 42 **(Right)** Detail of the biosensor from Fig. 41 shown in a section to reveal the width of the reed: by a special etching operation, this width is decreased by the amount δ, so that it can freely oscillate.

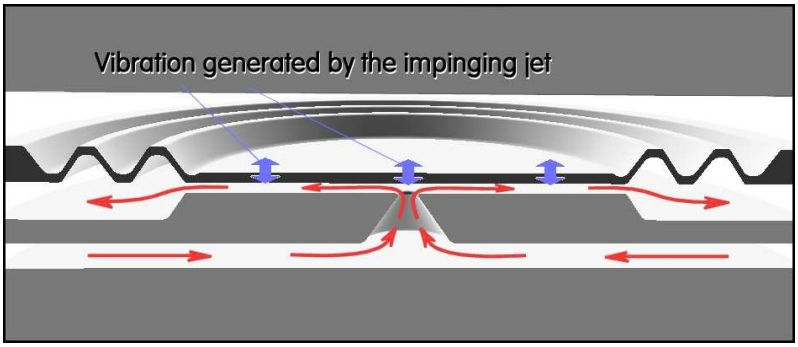

Fig. 43 Another possible layout of a micro-scale version of the "Aerodynamic Paradoxon" oscillator made by etching. In this case, the oscillator is of circular shape and the oscillating component with the detection surface is the membrane.

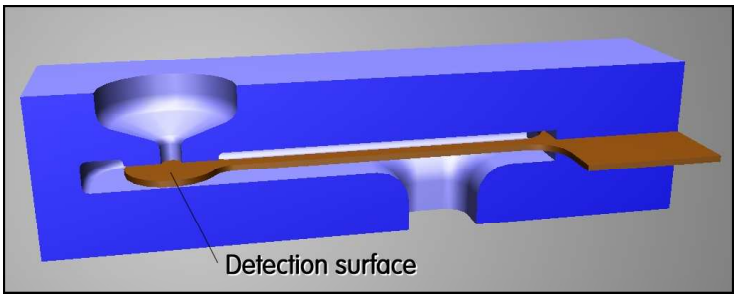

Fig. 44 Yet another possibility how to design the biosensor. The detection surface with the immobilised antibodies is the upper face of the disk held on a long cantilever.

in the fluid, it is separated, captured and held there. There are several variants how to detect the presence of the captured antigens. There are sensors relying on simple diffusion transport of the pathogens towards the detection surface – but this transport is very slow and ineffective at the small scales with absence of turbulence. A higher effectiveness is obtained by oscillating the fluid flow – or oscillating the detection surface. A particularly effective solution is oscillating the surface and at the same time employ the changes in the oscillation for the detection purposes. The mechanism off interest in the present context (Tesař, 2008) uses the change in the mass: the detection surface is arranged on an oscillating object and as the captured objects increase the mass of the object, the frequency of oscillation decreases. Of course, the oscillation of the object is a suitable field for applying the " Aerodynamic Paradoxon" effect.

In the example presented in Fig. 41, the detection surface is the surface of the reed facing the exit from the nozzle that is supplied with the fluid possibly containing the pathogens. The width of the reed is smaller – and indicated by the gap δ in Fig. 42 – than the thickness of the plate in which the cavities are made by etching. The added mass of captured pathogens on the reed decreases the frequency of the self-excited oscillation. Analogous alternative solutions are shown in the following illustrations Figs. 43 to 45. A particularly interesting alternative with oscillating hollow sphere as the contraction body located opposite to the surface S is presented in Fig. 45. It is very simple, since there is no need to guide the moving body by a spring or hinges. The antibodies are immobilised on the outer surface of the sphere – which is easily removable (by opening the top lid) for the purpose of the functionalising the surface.

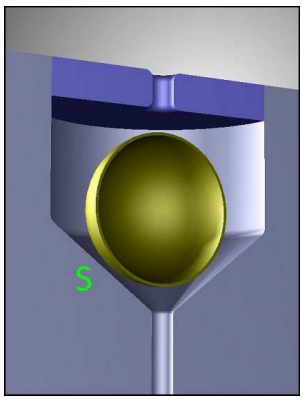

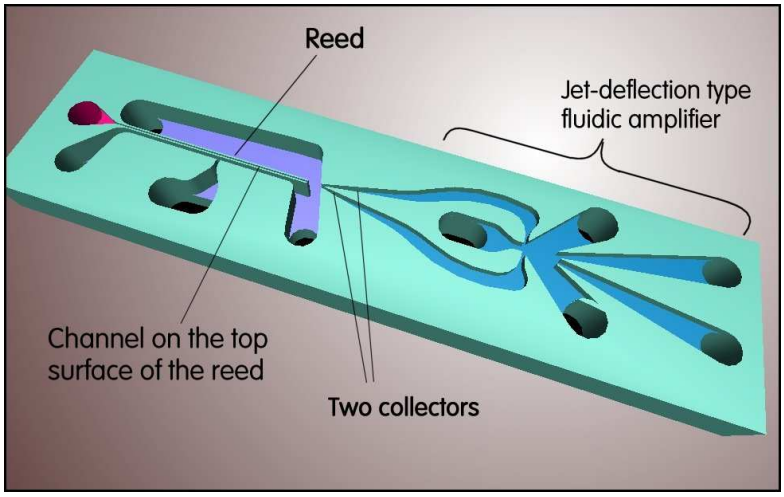

Fig. 45 **(Left)** The "Aerodynamic Paradoxon" effect may also generated between the conical surface S (replacing the plane surface S in Figs. 2 and 3) and the hollow sphere. The advantage is the sphere may be free - there is no necessity to restrain it by the spring or hinges.
Fig. 46 **(Right)** Fluidic detection of the reed motion: a fluid flows in the narrow channel etched on the top surface of the reed and after leaving the end of the reed is captured in the two collectors leading to the control nozzles of the fluidic amplifier.

There is, of course, a number of possibilities how to detect the change in frequency of the reed or contraction body. Fig. 41 uses the optical detection, Fig. 46 uses essentially the same configuration as in Fig. 41 with fluidic sensing (and fluidic amplification of the signal). The oscillatory motion of the sphere in Fig. 45 may be detected optically, the reed in Fig. 44 may be from a magnetic material so that its vibration may be sensed by a sensing coil.

8. An actuator: a very low speed fluid-driven motor

In designing the oscillating reed or the contraction body that in its oscillatory motion hits the opposing wall at a certain time in the oscillation cycle in the discussed devices an important aspect is securing proper conditions governing what happens after the first contact. Securing a long life of the moving component requires avoiding its tangential motion when in contact with the wall. If such a motion of the contact point (actually a small area) takes place, the reed surface may be soon worn out. Avoiding it calls for careful positioning of the reed percussion centre directly over the contact.

On the other hand, the tangential movement may be actually useful. They may be utilised in a class of devices that may be described as very simple pneumatic or hydraulic motors. With the wall replaced by a circumference of a wheel, as shown Fig. 18, the tangential motion causes the wheel to rotate. This, of course, may be made more effective if the percussion centre of the reed located far from the contact area. Even then the wheel rotation is slow and the generated torque available at the shaft of the wheel is small. There are, however, applications where these properties may represent an advantage. One of them is the use for activation of a bomb or a projectile. It is usually required that the bomb becomes ready to explode – initiated by a firing pin hitting an explosive substance – only after it travels a certain distance in the air. The usual way hot to secure this is to provide the bomb with a small propeller driven by the air flow past the bomb body. The propeller may be also

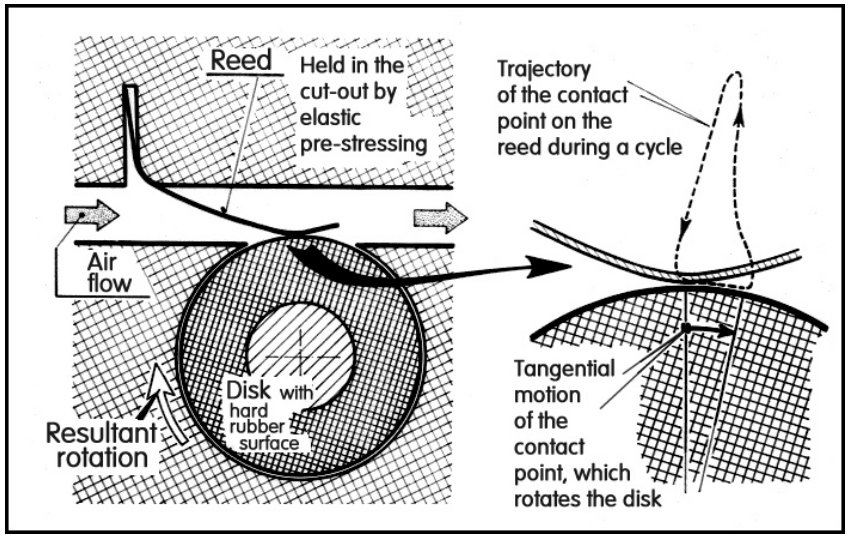

Fig. 47 If the contact point (in fact a small area) on the reed contacting the opposing wall does not coincide with the percussion centre, the contact surfaces experience a small tangential motion on impact. If the contact wall is replaced by the wheel (or disk), the tangential motion causes the wheel to rotate by a very small angle at each contact. The device operates an extremely simple, low-speed and low torque pneumatic motor.

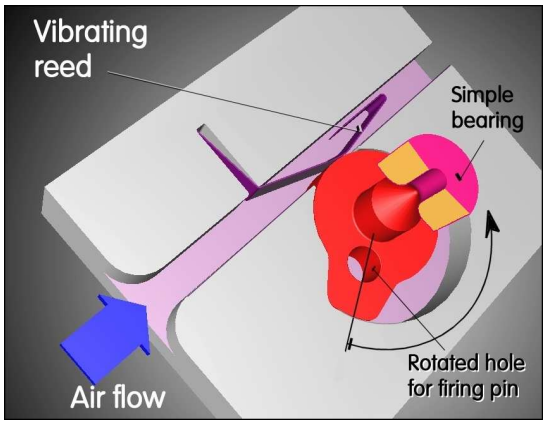

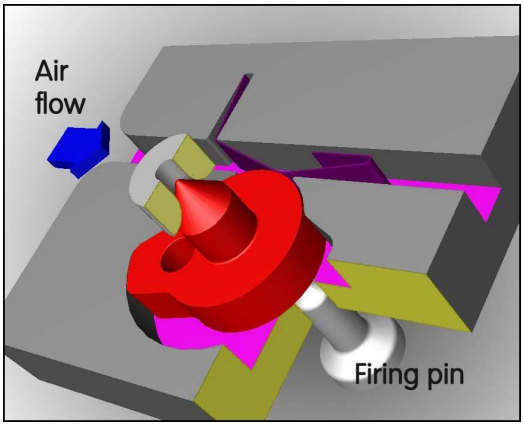

Fig. 48 (Left) The simple pneumatic motor may be used for activating a bomb. Note the end of the reed downstream from the contact point made heavy (by bending it bent back). This shifts the percussion centre to a different location relative to the constant than in Fig. 47. As a result, the disk rotates in a sense opposite to the one in Fig. 47.

Fig. 49 (Right) Another view of the simple activation mechanism from Fig. 48. It takes a considerable time for an air flow through the channel with the reed to move the red rotating part to the position at which it opens the path for the firing pin.

quite simple, but its disadvantage for this particular application is the relatively high rotation speed — while opening the hole for the firing pin to pass through requires only a short distance motion. In conventional bombs, this dilemma is solved by placing between the propeller and the arming mechanism a mechanical gear with extremely high speed reduction ratio. The gears, often arrange as multi-stage, are expensive. The pneumatic motor with the oscillating reed performs the task in an extremely simple and cheap manner. The air flow – perhaps from an intake at the bomb's nose – is led through the channel with the reed which it forces to oscillate. The mechanism being wholly inside the bomb body, it is less prone to being deformed and disabled than the delicate propeller.

8. Conclusions

The "Aerodynamic Paradoxon" effect - the of motion of a body (a free or supported disk or a flexible reed) in a direction opposite to what an uninitiated observer may intuitively expect - may give rise to vibration or oscillatory motion. This little known and so fat rarely if ever used mechanism is shown to offer several interesting application opportunities in fluidics.

Unfortunately, very little has been so far known about the theory of such oscillation. No analysis is available to the present author's knowledge, mainly because it is made rather difficult by the necessity to consider the impacts of the moving components (impact on the wall or mutual impact of two reeds in the symmetric versions). Also the reed shape variations during a cycle makes computations difficult. Even the experimental evidence is also far from satisfactory. Practically linear (but not proportional) dependences of the oscillation frequency on the flow rate (Fig. 11) and on the pressure (Figs. 31, 32) were both found. Many among the so far available experimental results show transitions between different regimes, called here M and N (Figs. 11, 15, 21, 26).

In view of the potential usefulness in fluidic applications – and the recently emerging microfluidic applications, in particular in biosensors - as well as the possibility of gaining an insight into other related fluid induced vibration, the absence of a deeper understanding is an obvious challenge.

Acknowledgement

The paper was written with the support by the grant Nr. 101/07/1499 donated by the Grant Agency of the Czech Republic. Support was also obtained from grant IAA200760705 granted by Grant Agency of the Academy of Sciences of the Czech Republic.

References

Clément N., Desormes C. (1827), Annales de Chimie et de Physique, Paris

Paivanas J.A., Hassan J.K. (1981) "*Attraction Force Characteristics Engendered by Bounded, Radially Diverging Air Flow*", IBM Journal of Research and Development, Vol. 25, No. 3

Tesař V. (1971) "*Generátor fluidických a/nebo elektrických pulsů*" (Generator of fluidic and/or electric pulses, in Czech), PV 6635-71, Czechoslovak Patent No. 148 721, 17th September 1971

Tesař V. (1972a) „*Převodník pro převod elektrického signálu na pulsně kódovaný signál fluidický*“ (Transducer for converting an electric signal into a pulse-coded fluidic signal – in Czech), PV 1381-72, Czechoslovak Patent No. 150 338, 2nd March 1972

Tesař V. (1972b) “*Převodník mechanického vstupního působení na pulsní fluidický výstupní signál*“ (Transducer of a mechanical input action into a pulse-type fluidic output signal – in Czech), PV 2513-72, Czechoslovak Patent No. 157 956, 4th April 1972

Tesař V. (1972c) “*Demodulátor pro zpracování frekvenčně modulovaného fluidického signálu*“ (Demodulator for processing a frequency modulated fluidic signal – in Czech), PV 2372-72, Czechoslovak Patent No. 155 582, 10th April 1972

Tesař V. (1972d) „*Mechanicko/fluidický převodník s pulsně zakódovaným výstupním signálem*“ (Mechano/fluidic transducer with pulse-coded output signal - in Czech), PV 2511-72, Czechoslovak Patent No. 155 583, 14th April 1972

Tesař V. (1972e) "*Fluidický teplomčrný prvek s frekvenčním výstupem*" (Fluidic thermometric element with frequency output – in Czech), PV 5343-72, Czechoslovak Patent No. 155 797, 31st July 1972

Tesař V. (1972f) "*Fluidický siloměrný snímač s vysokou vstupní mechanickou impedancí a pulsním výstupem*" (Fluidic sensor of mechanical force possessing a high mechanical input impedance and a pulse-type output – in Czech), PV 6221-72, Czechoslovak Patent No. 174 336, 11th September 1972

Tesař V. (1976) "*Nízkootáčkový pneumatický motorek pro malé výkony*" (Low-speed pneumatic motor for small outpur power levels – in Czech), PV 3946-76, Czechoslovak Patent No. 185 451, 15th June 1976

Tesař V. (2007) "*Pressure-Driven Microfluidics*", ISBN-10: 1596931345, Artech House Publishers, Norwood, MA 02062 USA, 2007

Tesař V. (2008) "*Čidlo částic nebo látek unášených tekutinou"* (Sensor for sensing particles or substances carried by a fluid – in Czech), Patent Application Nr. PV 2008-140, Czech Patent Office, 7th March 2008

Tesař V., Balda M. (1972) "*Fluidický prvek se třemi zíkladními vývody, zejména použitelný jako generátor fluidických pulsů*" (A fluidic element possessing three basic terminals, particularly useful as a generator of fluidic pulses – in Czech), PV 1865-72, Czechoslovak Patent No. 158 104, 20th March 1972

Teyssler V., Kotyška V. (1933) „*Technický slovník naučný*" (Encyclopaedia of technology – in Czech), Volume IX, p. 929, Borský a Šulc publishers, Prague

Antoine M., Hemon P., de Langre E. (2008) "*Aeroelastic instability of plate subject to normal jet*", Proc. of 9th Int. Conference on Flow-Induced Vibrations, Prague, Czech Republic